Arch. Metall. Mater. **63** (2018), 2, 809-816

DOI: 10.24425/122407

N. RADEK*, A. SZCZOTOK**, A. GĄDEK-MOSZCZAK***, R. DWORNICKA****,
J. BRONČEK*****, J. PIETRASZEK****,#

THE IMPACT OF LASER PROCESSING PARAMETERS ON THE PROPERTIES OF ELECTRO-SPARK DEPOSITED COATINGS

The paper described properties of electro-spark deposited coatings under influence of the laser treatment process. The properties were assessed by analyzing the coating microstructure, X-ray radiation, microhardness, bonding strength, corrosion resistance, porosity and wear tests. The tests were conducted for Mo and Cu coatings (the anode) which were electro-spark deposited over the C45 steel substrate (the cathode) and melted with a laser beam. The coatings were deposited by means of an ELFA-541. The laser processing was performed with an Nd:YAG laser. The coatings after laser processing are still distinguished by very good performance properties, which make them suitable for use in sliding friction pairs.

Keywords: electro-spark deposition, laser treatment, material properties, coating, design of experiments

1. Introduction

By applying new engineering materials or protective coatings, it is possible to improve the functional properties of machine parts so that they are resistant to corrosion, abrasion and erosion, and possess high fatigue strength. The new materials, for instance, alloy steels, are usually costly, which is undesirable, because the higher the cost of the material, the higher the price of a finished product. However, if an element is to be subjected to high loads, then strength rather than cost is a primary factor.

Applying protective coatings to machine parts is economically justifiable if the wear is local or if the coating material is expected to display properties different from those of the substrate. Most surface layers are technological surface layers (TSLs) – they are produced before objects are used. Functional surface layers (FSLs), on the other hand, are applied during maintenance.

Depositing protective layers on metal surfaces frequently involves matter and energy transfer, which is accompanied by various chemical, electrochemical and electrothermal reactions. To determine the operational properties of a surface layer, it is necessary to analyze the original, technological properties of the material, the deposition method, and, particularly, the mechanism of energy accumulation inside and outside the workpiece.

By controlling polarity, it is possible to remove or replace material. The process of material removal involving erosion of the stock subjected to electric discharges is called electrical discharge machining (EDM). The surface layer forming on the product improves its operational properties.

The process of material growth resulting from electroerosion is known as elektro-spark alloying (ESA) or electro-spark deposition (ESD). The erosion of the anode and the spark discharges between the electrodes result in the formation of a surface layer with properties different from those of the base material [1-4].

An alternative to the use of ESD technologies steels with different properties [5-8].

Electro-spark deposited coatings have some disadvantages but these can be easily eliminated. One of the methods is laser beam machining (LBM); a laser beam is used for surface polishing, surface geometry formation, surface sealing or for homogenizing the chemical composition of the deposited coatings [9-12].

It is envisaged that the advantages of laser-treated electro-spark coatings will include:

- lower roughness,
- lower porosity,
- better adhesion to the substrate,
- higher wear and seizure resistance,
- higher fatigue strength due to the occurrence of compressive stresses on the surface,
- higher resistance to corrosion.

* KIELCE UNIVERSITY OF TECHNOLOGY, CENTRE FOR LASER TECHNOLOGIES OF METALS, AL. 1000-LECIA PAŃSTWA POLSKIEGO 7, 25-314 KIELCE, POLAND
** SILESIAN UNIVERSITY OF TECHNOLOGY, FACULTY OF MATERIALS SCIENCE AND METALLURGY, INSTITUTE OF MATERIALS SCIENCE, 8 KRASIŃSKIEGO STR., 40-019 KATOWICE, POLAND
*** CRACOW UNIVERSITY OF TECHNOLOGY, FACULTY OF MECHANICAL ENGINEERING, AL. JANA PAWŁA II 37, 31-864 CRACOW, POLAND
**** CRACOW UNIVERSITY OF TECHNOLOGY, DEPARTMENT OF SOFTWARE ENGINEERING AND APPLIED STATISTICS, AL. JANA PAWŁA II 37, 31-864 CRACOW, POLAND
***** UNIVERSITY OF ZILINA, UNIVERZITNA 1, 01-026 ZILINA, SLOVAKIA

Corresponding author: pmpietra@gmail.com

2. Materials and methods

2.1. Coating

The tests were conducted for Cu-Mo coatings produced by electro-spark deposition, which involved applying Cu and Mo electrodes with a diameter of 1 mm (the anode) on the C45 steel substrate (the cathode). Here copper constitutes the core coating material in the formation of low-friction surface layers; it also compensates for the occurrence of residual stresses. Molybdenum act as the reinforcing constituents. The coating materials, i.e. molybdenum (99.8% Mo) and copper (99.2% Cu) in the form of wire (ϕ = 1 mm) were purchased from BIBUS Metals Sp. z.o.o. (certificate included).

2.2. Deposition

The coatings were electro-spark deposited on C45 steel substrate by means of the ELFA-541 made by a Bulgarian manufacturer. Base on the analyses of the current characteristics as well as the manufacturer's recommendations, it was assumed that the parameters of the ESD operation should be as follows: current intensity I = 16 A (for Cu I = 8A); table shift rate v = 0.5 mm/s; rotational speed of the head with electrode n = 4200 rev/min; number of coating passes L = 2; capacity of condenser system C = 0.47 μF; pulse duration T_i = 8 μs; interpulse period T_p = 32 μs; frequency f = 25 kHz.

2.3. Laser treatment

The subsequent laser treatment was performed with the aid of a BLS 720 laser system employing the Nd:YAG laser operating in the pulse mode. The following parameters were assumed for the laser treatment: laser spot diameter d = 0.7 mm; laser power P = 20 W; beam shift rate v = 250 mm/min; nozzle-sample distance h = 1 mm; pulse duration t_i = 0.4 ms; frequency f = 50 Hz.

2.4. Microstructure and X-ray radiation analysis

A Joel JSM-5400 scanning microscope equipped with an Oxford Instruments ISIS-300 X-ray microanalyzer was used to test the coating microstructure.

2.5. Corrosion resistance tests

The corrosion resistance [13] of the Cu-Mo coating and the underlying substrate before and after laser treatment was analyzed using a computerized system for electrochemical tests, Atlas'99, produced by Atlas-Sollich. The potentiodynamic method was applied, because it is reported to be one of the most effective methods of electrochemical testing.

The cathode polarization curve and the anode polarization curve were determined by polarizing the samples with a potential shift rate of 0.2 mV/s in the range of ±200 mV of the corrosive potential, and with 0.4 mV/s in the range of higher potentials. Samples with a marked area of 10 mm in diameter were polarized up to a potential of 500 mV. The polarization curves were drawn for samples exposed for 24 hours to a 3.5% NaCl solution so that the corrosive potential could be established. The tests were performed at a room temperature of 21°C (±1°C).

2.6. Adhesion and microhardness tests

A scratch test was conducted to measure the adhesion of the Cu-Mo coatings before and after laser treatment. A CSEM REVETEST scratch tester was used. The measurements were performed at a load increase rate of 103.2 N/min, a table feed rate of 9.77 mm/min and a scratch length of 9.5 mm.

A special indentor – a Rockwell diamond cone with a corner radius of 200 mm, was used to scratch the samples at a gradually increasing normal force (load). The information about the cracking or peeling of layers was obtained basing on the measurements of the material resistance (tangential force) and the registration of acoustic emission signals. The lowest normal force causing a loss of adhesion of the coating to the substrate is called critical force and is assumed to be the measure of adhesion.

The critical force was determined basing on the records of changes in the acoustic emission signals and the tangential force as well as on the results of observations with an optical microscope fitted in the REVETEST tester. The values of the critical force were established by comparing the scratches left by the indentor with the responses of acoustic emission signals.

The microhardness was determined by using the Vickers method (Hanemann tester). The measurements were performed under a load of 0.4 N. The indentations were made in perpendicular microsections in three zones: the white homogeneous difficult-to-etch coating, the heat affected zone (HAZ) and the substrate.

2.7. Porosity measurements

For assess the degree of porosity of the coatings tested WC-Cu before and after laser treatment, quantitative image analysis was performed using software supplied with the SIS which (SEM) Philips XL30 / LaB6. In the analysis guided by the principle of Cavalieri-Hacquerta according to which, a measure of the porosity can be shares of the pores:

- volume (the ratio of the total volume of voids to the total volume of the fragment of the coating);
- surface (the ratio of the total pore area to the total area analyzed grinding);
- the length of the control section (the ratio of the total length of the strings passing through the pores of the length of the analyzed section of the measurement plane grinding).

2.8. Texturing methodology and wear tests

Laser surface texturing is one of the most common and promising methods of surface roughening. Categorized as a metal removal process, laser texturing is usually performed at a power density of $10^6 \div 10^9$ W/cm^2. At present, it accounts for about 2% of all laser-based material processing processes used in the world [14-16].

In laser surface texturing, a pulsed laser beam is focused on a material to melt a hole. The hole depth is dependent mainly on the power density and the pulse duration. The drilling debris is removed from a hole being drilled using compressed air or another inert gas.

The texturing was performed using an Nd:YAG laser (impulse mode), model BLS 720, and operating in the pulse mode under the following conditions: laser spot diameter $d = 0.7$ mm; laser power $P = 20$ W; beam shift rate $v = 1200$ mm/min; nozzle-sample distance $h = 1$ mm; pulse duration $t_i = 1.2$ ms; frequency $f = 8$ Hz.

A Joel JSM-5400 scanning electron microscope was used to study the effects of laser surface texturing.

The wear tests of the Cu-Mo electro-spark deposited coatings before and after laser surface texturing were carried out using the pin-on-disc tester T-01M [17].

The tester makes it possible to measure the friction force for a predetermined load. The pin $\phi 4 \times 20$ mm was made of tool steel. The samples and anti-samples were prepared in accordance with the instruction. The tests were conducted at the following parameters of friction: linear velocity $v = 0.8$ m/s; test duration $t = 3600$ s; sliding distance $S = 2880$ m; range of load changes: 5, 10, 15 N.

A drop of lubricant-paraffin oil was applied on the ring raceway only once. It was necessary to measure the time after which the value of the friction coefficient increased.

2.9. Statistical analysis

The wear tests were performed according to a typical experimental design [18] with three factors (a laser treatment, a lubrication and a geometric form) at two levels and one factor (a load) at three levels. Only one measurement per a treatment was made i.e. there are no additional replications. The outcome was a mass loss.

The friction coefficient tests were performed according to a typical experimental design [18] with two factors (a laser treatment and a lubrication) at two levels and one factor (a load) at three levels. Only one measurement per a treatment was made i.e. there are no additional replications. The outcome was a friction coefficient.

First, the raw effect analysis [19,20] was performed to reveal the impact of single factors and their interactions on the outcome. The second setting of the load was ignored during this step of the analysis. The tail of the resulted histogram may be ignored in the further analysis allowing to evaluate the residual error and related p-values [21]. In the second step, the analysis of variance (ANOVA) [19,22] with interactions up to second order was performed.

3. Results and discussion

3.1. Microstructure and x-ray radiation analysis

Figures 1a show the microstructure of electro-spark deposited two-layer Cu-Mo coating. The layer thickness is approximately 8÷10 μm, and the range of the heat affected zone (HAZ) inside the (underlying) substrate material is about 10÷15 μm. In the photograph, the boundary line between the two-layer coating and the substrate is clear. There are microcracks running across and along the coating. A linear analysis of the elements (Fig. 1b) of the Cu-Mo coating shows that the distribution of elements is non-uniform; there are zones with greater concentrations of Cu, Mo and Fe. Analyzing the linear distribution of elements, one can see that the adhesion of the coating to the substrate is of dif-

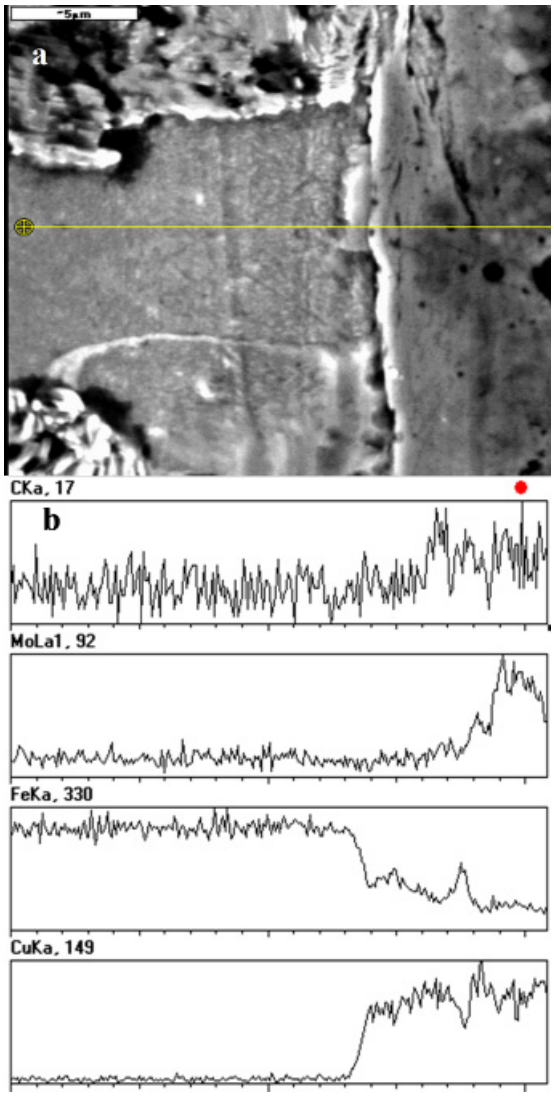

Fig. 1. Microstructure (a) and linear distribution of elements (b) in the Cu-Mo coating (scale marker: 5 μm)

fusive type. There is no clear separation of components in the Cu-Mo coating (Fig. 1b). A higher content of carbon reported in the electro-spark deposited Cu-Mo coating is a result of diffusion. Carbon from the C45 steel substrate travels to the electro-spark deposited technological surface layer (TSL) because of thermal interaction.

The melting and solidification processes during laser treatment resulted in the migration of elements across the coating-substrate interface. Laser radiation caused intensive convective flow of the liquid material in the pool and, in consequence, the homogenization of the chemical composition (Fig. 2b). It also led to the structure refinement and highly saturated phase crystallization (Fig. 2a) because of considerable gradients of temperature and high cooling rates. The technological surface layers, produced by laser alloying, were free from microcracks and pores – an effect of surface sealing, and non-continuities across the coating-substrate interface. The thickness of the fused two-layer Cu-Mo coating ranged 20÷40 μm. In the heat affected zone (HAZ), which was 20÷50 μm thick, there was an increase in the content of carbon (Fig. 2b).

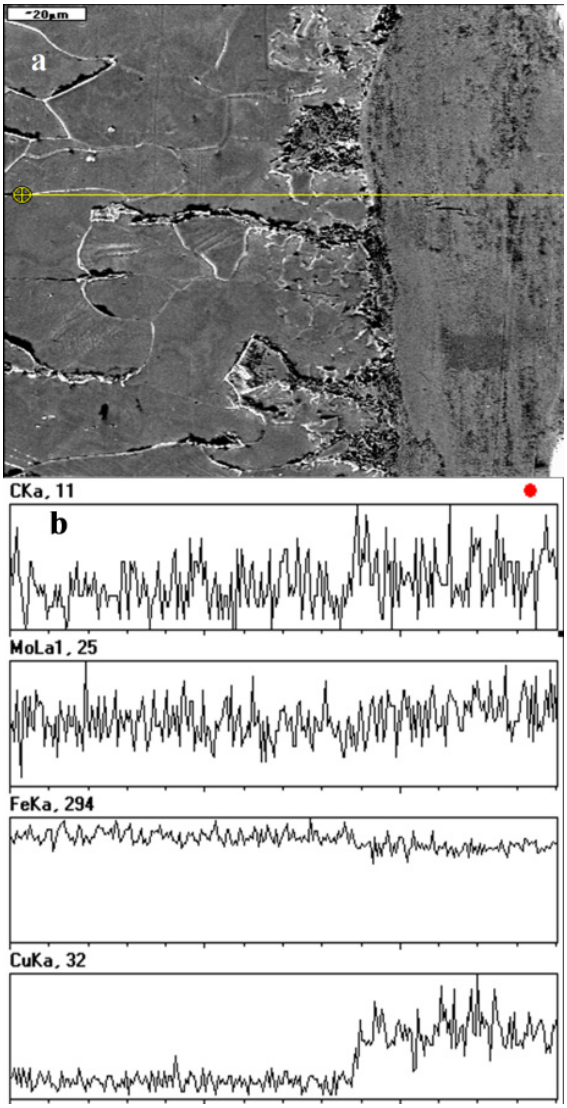

Fig. 2. Microstructure (a) and linear distribution of elements (b) in the Cu-Mo coating after laser treatment (scale marker: 20 μm)

The point analysis conducted for the outer surface of the technological surface layers (Fig. 3a) shows high intensity of peaks of the elements present in the coating. The Cu-Mo coating contained 66.07% at. of Cu and 10.98% at. of Mo, which may testify to the mixing of the two elements and the formation of a multi-phase alloy (Fig. 3a).

The point analysis of the electro-spark coatings treated with a laser beam (Fig. 3b) shows high intensity of iron peaks in the alloyed layers. The content of iron in the laser-treated technological surface layers was between 88% at. and 97% at. After laser treatment, the intensity of Mo and Cu peaks in the electro-spark deposited coatings was lower.

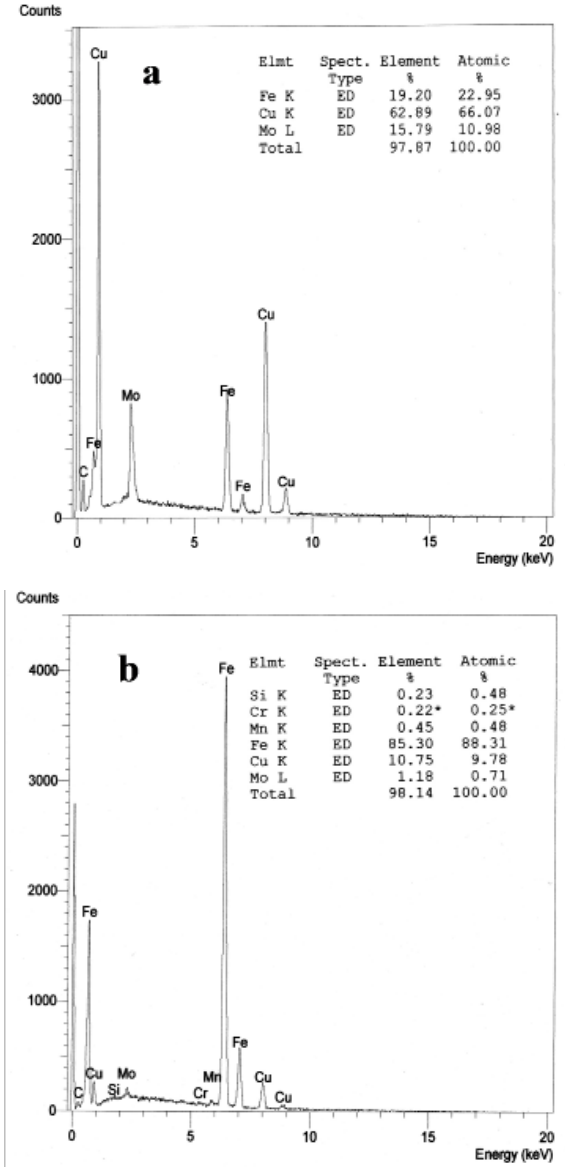

Fig. 3. Spectrum of an X-ray radiation for an electro-spark deposited Cu-Mo coating on a C45 steel substrate: a) before laser treatment; b) after laser treatment

3.2. Corrosion resistance tests

The characteristic electrochemical values of the materials under test are presented in Table 1. The electro-spark deposited

coatings were reported to have similar corrosion resistance to that of the substrate material. A system with a two-layer coating is assumed to fulfill two functions: increase corrosion resistance and wear resistance. The coatings which contained Cu acted as cathodes. Resistance to wear and corrosion depends on the quality of coatings, particularly their sealing properties.

TABLE 1

Current density and corrosion potential of the materials tested

Material	Corrosion current density I_k [μA/cm^2]	Corrosion potential E_{KOR} [mV]
C45	112 ± 17.8%	–458
C45 + laser	86.4 ± 16%	–522
Cu-Mo	42.9 ± 11.8%	–620
Cu-Mo + laser	30.7 ± 2.6%	–629

The Cu-Mo coating was reported to have the highest corrosion resistance. The corrosion current density of the coating was 42.9 μA/cm^2, while that of the C45 steel substrate was 112 μA/cm^2. Applying the Cu-Mo coating improved the sample corrosion resistance by approx. 162%. There was some improvement in the corrosion resistance of the electro-spark deposited coatings after laser treatment. The healing of microcracks resulted in higher density and therefore better sealing properties. The highest corrosion resistance after laser treatment was reported for the Cu-Mo coating (I_k = 30.7 μA/cm^2). For the C45 steel substrate, I_k was 6.4 μA/cm^2. Thus, the corrosion resistance increased by about 30% after laser treatment. Laser treatment improved the surface smoothness and corrosion resistance; there was a decrease in the surface roughness, Ra, from 2.02 μm to 1.75 μm.

3.3. Adhesion and microhardness tests

Table 2 shows the values of the critical force obtained from three measurements of a given sample, the force mean values and standard deviations.

TABLE 2

Results of the adhesion test

Coating	Critical force [N]			Mean value [N]	Standard deviation [N]
	Measurement number				
	1	2	3		
Cu-Mo	4.34	4.59	2.82	3.91	0.95
Cu-Mo + laser	5.91	4.78	5.15	5.28	0.57

Laser-treated coatings produced by electro-spark alloying are reported to possess adhesion higher than untreated coatings. The mean value of the critical force of the Cu-Mo coating calculated from three measurements was 3.91 N; after laser treatment, it increased to 5.28 N. The treatment caused a 26% improvement in the adhesion of the Cu-Mo coating. The higher adhesion of coatings subjected to laser treatment was probably due to their lower porosity related to higher sealing properties. Further details, however, will be established in the next stage of the research.

The microhardness test results for the electro-spark deposited Cu-Mo coating before and after laser treatment are shown in diagrams in Fig. 4. Electro-spark deposition caused changes in the microhardness of the material. The microhardness of the substrate after electro-spark deposition was on average 281 HV0.4; the same value was reported for the substrate before the process. There was a considerable increase in microhardness after depositing the heterogeneous Cu-Mo coating. The microhardness of the Cu-Mo coating was approx. 587 HV0.4, which gives increase of 110%. The microhardness of the Cu-Mo coating in the heat affected zone (HAZ) after electro-spark treatment was 51% higher than that of the substrate material. Laser treatment had a favorable effect on the changes in the microhardness of the electro-spark deposited of the Cu-Mo coating. There was an increase of 161% in the microhardness of the Cu-Mo coating.

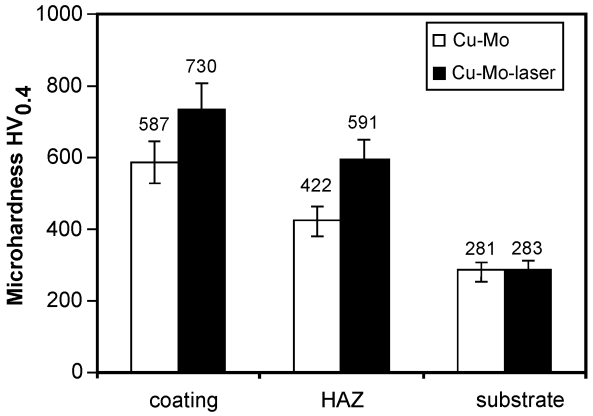

Fig. 4. Results of the microhardness tests for the Cu-Mo coating before and after laser treatment

3.4. Porosity measurements

Results of the surface porosity for the Cu-Mo coating before and after laser treatment are shown in Table 3.

TABLE 3

Results of the surface porosity for the Cu-Mo coating before and after laser treatment

Coating	Porosity [%]			Mean value [%]	Standard deviation [%]
	Measurement number				
	1	2	3		
Cu-Mo	4.2	3.7	2.9	3.6	0.7
Cu-Mo + laser	0.1	0.2	0.1	0.13	0.06

Analyzing the table it can be seen that the applied coatings have a higher porosity with respect to the coating after laser treatment. Laser treatment reduced the porosity of the coatings more than 20 times. The porosity of the coatings Cu-Mo was located in the range of 2.9÷4.2%, and after laser treatment was

0.1÷0.2%. Lower porosity of the Cu-Mo coatings by positive influence on their performance characteristics, improving their corrosion resistance, adhesion and microhardness.

3.5. Texturing and wear tests

Selected SEM images are presented in Fig. 5 and Fig. 6. As can be seen, the surface structure after laser surface texturing is regular. The surface is covered by bumps and dimples resulting from phase and structural modifications and the accompanying specific volume changes in the laser affected zones. Lapping and super finish are used to obtain hard flat areas transferring normal loads and areas of pores where the hydrodynamic forces are generated during fluid lubrication. Surfaces with such a texture can be applied, for instance, to sliding friction systems. The microscopic analysis showed that the removal of the drilling debris was not complete when the laser beam was focused locally. This was probably due to insufficient power density. The action of the thermocapillary forces and the convective motion resulted in the formation of rims, whose structure consisted of molten and then crystallized Cu-Mo.

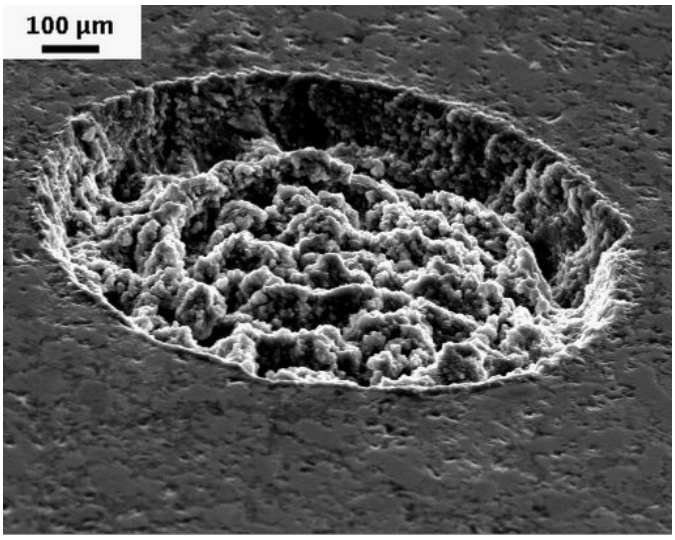

Fig. 5. A single microcavity on the ring

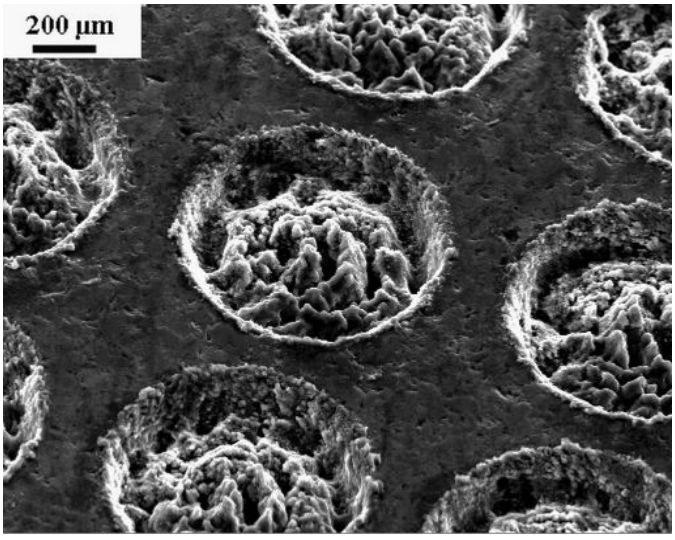

Fig. 6. A system of microcavities on the ring

The wear test results for the electro-spark deposited Cu-Mo coating before and after laser surface texturing are shown in Table 4 and Table 5. Table 6 shows the values of the friction coefficient for the Cu-Mo coating before and after laser surface texturing.

TABLE 4

Results of the wear test for the Cu-Mo coating before laser surface texturing

Load [N]	Mass loss [mg]			
	not lubricated		lubricated oil	
	pin	disc	pin	disc
5	6.16	9.64	4.89	6.33
10	13.05	16.84	9.06	11.54
15	19.41	23.28	13.14	18.67

TABLE 5

Results of the wear test for the Cu-Mo coating after laser surface texturing

Load [N]	Mass loss [mg]			
	not lubricated		lubricated oil	
	pin	disc	pin	disc
5	5.44	6.88	3.35	4.26
10	10.24	12.16	7.11	8.63
15	14.88	20.16	10.29	15.72

TABLE 6

Results of the friction coefficient for the Cu-Mo coating before and after laser surface texturing

Load [N]	Friction coefficient			
	not lubricated		lubricated oil	
	Cu-Mo	CuMo+laser	Cu-Mo	Cu-Mo+laser
5	0.39	0.33	0.21	0.14
10	0.54	0.46	0.35	0.23
15	0.67	0.48	0.43	0.32

3.6. Statistical analysis results

The dataset obtained during wear tests are presented in both Table 4 and Table 5. The dataset obtained during friction coefficient tests are presented in Table 6.

The raw effects analysis of the mass loss and the resulted Pareto chart (Fig. 7) revealed that the impact of the load dominates, then equivalently the impact of the lubrication and the impact of the geometric form and slightly weaker the impact of the laser treatment. The fact that linear effects dominates (i.e. all interactions are weaker than linear effects) is very important for the potential optimization of a technological processes because it means that each factor may be optimized separately.

The further ANOVA analysis of the mass loss (Table 7) showed that – apart of linear effects – two second order interactions are statistically significant: the load with the lubrication and the load with the geometric form however their significance is weaker than linear effects. It means that they should be considered in the prediction model but the optimization may be processed for each of the factors separately.

TABLE 7

ANOVA results for the mass loss (acronyms [22]: SS – sum of squares; df – degrees of freedom; MS – mean square; F – Fisher's statistics; p – critical significance level)

Effect	SS	df	MS	F	p
Constant term	3062.978	1	3063	7122	0.000
Laser	45.073	1	45.1	105	0.000
Load	491.195	2	246	571	0.000
Lubrication	84.938	1	84.9	198	0.000
Form	57.320	1	57.3	133	0.000
Laser*Load	2.889	2	1.44	3.36	0.081
Laser*Lubrication	0.788	1	0.788	1.83	0.209
Load*Lubrication	7.201	2	3.60	8.37	0.009
Laser*Form	0.697	1	0.697	1.62	0.235
Load*Form	11.624	2	5.81	13.5	0.002
Lubrication*Form	0.254	1	0.254	0.59	0.462
Error	3.870	9	0.430		

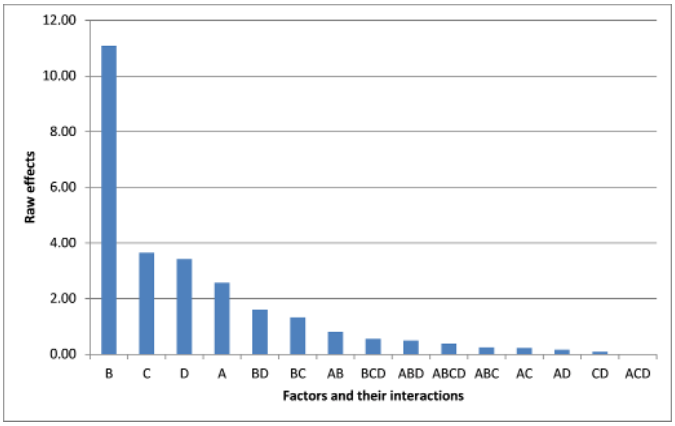

Fig. 7. Pareto chart for the raw effects analysis of the mass loss. Codes: A – a laser treatment (yes vs. no), B – a load (5 N vs. 15 N), C – a lubrication (nothing vs. oil), D – a geometric form (pin vs. disc); multi-characters – respective interactions

The raw effects analysis of the friction coefficient and the resulted Pareto chart (Fig. 8) revealed that the impact of the load dominates equivalently with the impact of the lubrication while the impact of the laser treatment is a half of them. The fact that linear effects dominates (i.e. all interactions are weaker than linear effects) is very important for the potential optimization of a technological processes because it means that each factor may be optimized separately.

The further ANOVA analysis of the mass loss (Table 8) showed that only linear effects are statistically significant.

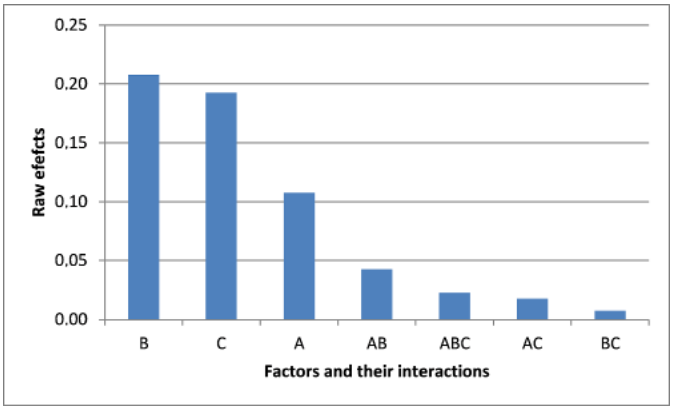

Fig. 8. Pareto chart for the raw effects analysis of the friction coefficient. Codes: A – a laser treatment (yes vs. no), B – a load (5 N vs. 15 N), C – a lubrication (nothing vs. oil); multi-characters – respective interactions

TABLE 8

ANOVA results for the friction coefficient (acronyms [22]: SS – sum of squares; df – degrees of freedom; MS – mean square; F – Fisher's statistics; p – critical significance level)

Effect	SS	df	MS	F	p
Constant term	1.725208	1	1.73	1769	0.001
Load	0.087617	2	0.044	44.9	0.022
Lubrication	0.118008	1	0.118	121	0.008
Laser	0.033075	1	0.033	33.9	0.028
Load*Lubrication	0.000317	2	0.000158	0.162	0.860
Laser*Load	0.003650	2	0.001825	1.87	0.348
Laser*Lubrication	0.000075	1	0.000075	0.077	0.808
Error	0.001950	2	0.000975		

4. Conclusions

The following conclusions can be drawn from the analysis and test results.

1. A concentrated laser beam can effectively modify the state of the surface layer, i.e. the functional properties of electro-spark coatings.
2. Laser radiation causes an improvement in the functional properties of the two-layer electro-spark deposited Cu-Mo coatings, i.e. they exhibit higher microhardness and higher resistance to adhesion and corrosion.
3. There is no change in the chemical composition of electro-spark deposited coatings after laser treatment in spite of their melting and solidification. The results of the laser radiation are the homogenization of the chemical composition, structure refinement and the healing of microcracks and pores.
4. Coatings after laser treatment are less porosity (more than 26 times).
5. Laser texturing of Cu-Mo coatings provides increased resistance to wear and reducing of friction coefficient.
6. The surface structure after laser surface texturing (i.e. the microcavities) is desirable in sliding friction pairs. They

may be used as reservoirs of lubricants as well as sources of hydrodynamic forces increasing the capacity of a sliding pair.

7. Statistical analysis revealed that laser treatment is not dominantly confounded with other technological factors (interactions are weaker than any linear effect) i.e. the laser treatment may be optimized independently from other factors.
8. In the next phase of the research, it is essential to determine the phase composition Cu-Mo of the coatings before and after laser treatment.
9. It seems that one should use more sophisticated, but also more computationally expensive statistical non-parametric methods [23,24] in further investigation to reveal relationships between factors deeper than it is possible in a classic statistical analysis [25-27], however the computational cost of such enhancement is very high [21]. It may include specific non-parametric methods for the analysis of multidimensional sparse and uncertain data [28] (e.g. porous sinterings [29-31] or other porous media [32]), advanced image analysis methods [33,34] and the fuzzy statistics for the selection of dominant factors, derived from a production engineering [35-37].

REFERENCES

[1] A. Agarwal, N.B. Dahotre, Surf. Coat. Tech. **106**, 242-250 (1998).
[2] B. Antoszewski, E. Evin, J. Audy, J. Tribol.-Trans. ASME **3**, 253-262 (2008).
[3] A.V. Ribalko, O. Sahin, Surf. Coat. Tech. **168**, 129-135 (2003).
[4] C.B. Tang, D.X. Liu, Z. Wang, Y. Gao, Appl. Surf. Sci. **257**, 6364-6371 (2011).
[5] W. Kwaśny, T. Jung, Technical Trans. **2-M**, 119-124 (2015).
[6] J. Lubas, Technical Trans. **7-M**, 295-301 (2008).
[7] R. Ulewicz, J. Balk. Tribol. Assoc. **21**, 166-172 (2015).
[8] R. Ulewicz, F. Novy, J. Selejdak, Adv. Mater. Res.-Switz. **874**, 43-48 (2014).
[9] A. Gadek-Moszczak, N. Radek, S. Wronski, J. Tarasiuk, Adv. Mater. Res.-Switz. **874**, 133-138 (2014).
[10] J. Pietraszek, N. Radek, K. Bartkowiak, Solid State Phenom. **197**, 198-202 (2013).
[11] N. Radek, J. Konstanty, Arch. Metall. Mater. **57**, 665-670 (2012).
[12] N. Radek, E. Wajs, M. Luchka, Powder Metall. Met. C+ **47**, 197-201 (2008).
[13] M. Scendo, J. Trela, N. Radek, Surf. Coat. Tech. **259**, 401-407 (2014).
[14] B. Antoszewski, Adv. Mater. Res.-Switz. **874**, 51-55 (2014).
[15] G. Ryk, I. Etsion, Wear **261**, 792-796 (2006).
[16] W. Yi, X. Dang-Sheng, J. Mater. Process. Tech. **197**, 96-100 (2008).
[17] N. Radek, J. Pietraszek, B. Antoszewski, Adv. Mater. Res.-Switz. **874**, 29-34 (2014).
[18] O. Kempthorne, K. Hinkelmann, Design and analysis of experiments. Vol. 1. Introduction to experimental design, John Wiley & Sons, Hoboken, NJ, USA (2007).
[19] T.P. Ryan, Modern Experimental Design, John Wiley & Sons, Hoboken (2007).
[20] J. Pietraszek, A. Gadek-Moszczak, T. Torunski, Adv. Mater. Res.--Switz. **874**, 139-143 (2014).
[21] Y. Pawitan, In All Likelihood: Statistical Modelling and Inference Using Likelihood, Clarendon Press, Oxford (2001).
[22] D.C. Montgomery, Design and Analysis of Experiments, John Wiley & Sons, Inc., Hoboken (2008).
[23] A.B. Owen, Empirical Likelihood, Chapman & Hall/CRC, Boca Raton (2001).
[24] E. Skrzypczak-Pietraszek, I. Kwiecien, A. Goldyn, J. Pietraszek, Phytochem. Lett. **20**, 443-448 (2017).
[25] R. Dwornicka, Adv. Mater. Res.-Switz. **874**, 63-69 (2014).
[26] U. Ferdek, M.S. Kozien, Acta Phys. Pol. A **123**, 1044-1047 (2013).
[27] L. Skrzypczak, E. Skrzypczak-Pietraszek, E. Lamer-Zarawska, B. Hojden, Acta Soc. Bot. Pol. **63**, 173-177 (1994).
[28] A. Szczotok, M. Sozanska, Prakt. Metallogr.-Pr. M. **46**, 454-468 (2009).
[29] F. Deflorian, L. Ciaghi, J. Kazior, Werkst. Korros.-Mater. Corros. **43**, 447-452 (1992).
[30] M. Hebda, S. Gadek, J. Kazior, J. Therm. Anal. Calorim. **108**, 453-460 (2012).
[31] A. Tiziani, A. Molinari, J. Kazior, G. Straffelini, Powder Metall. Int. **22**, 17-19 (1990).
[32] T. Wejrzanowski, S. Haj Ibrahim, J. Skibinski, K. Cwieka, K.J. Kurzydlowski, Image Anal. Stereol. **36**, 105-110 (2017).
[33] A. Gadek-Moszczak, J. Pietraszek, B. Jasiewicz, S. Sikorska, L. Wojnar, Stud. Comput. Intell. **572**, 127-136 (2015).
[34] J. Korzekwa, A. Gadek-Moszczak, M. Bara, Prakt. Metallogr.--Pr. M. **53**, 36-49 (2016).
[35] A.V. Goroshko, V.P. Royzman, A. Bubulis, K. Juzenas, J. Vibroeng. **16**, 2178-2187 (2014).
[36] A. Szczotok, Materialwiss. Werkst. **46**, 320-329 (2015).
[37] A. Goroshko, V. Royzman, V. Ostasevicius, Mechanika **22**, 206-211 (2016).